© Med Sci Monit, 2011; 17(12): BR377-384
PMID: 22129896

Received: 2011.03.22
Accepted: 2011.05.23
Published: 2011.12.01

Autologous nerve implantation into denervated monkey skin promotes regeneration of Meissner's corpuscle

Authors' Contribution:
A Study Design
B Data Collection
C Statistical Analysis
D Data Interpretation
E Manuscript Preparation
F Literature Search
G Funds Collection

Zhen-Xiang Wang[1A*], Dong-Lin Luo[2A*], Pan Yu[1C], Liang Chen[1B], Zhe Li[1C], Ling Tao[1D], Xia Dai[1F], Yue-Jun Li[1E], Xue-Yong Li[1C], Shi-Rong Li[1G]

[1] Department of Plastic Surgery, Southwest Hospital, 3rd Military Medical University, Chongqing, China
[2] Department of General Surgery, Institute of Battle Surgery Research, Daping Hospital, 3rd Military Medical University, Chongqing, China

* Zhen-Xiang Wang and Dong-Lin Luo contributed equally to this study

Source of support: Departmental sources

Summary

Background: The aim of this study was to observe the effects of autologous nerve implantation into the denervated finger flap on the regression and regeneration of sensory nerve endings and Meissner's corpuscles.

Material/Methods: Bilateral nerves of fingers were separated: one was removed and the other was implanted into the denervated finger in the implantation group. In the non-implantation group, both nerves were removed. The ventral skin of fingers was collected for immunohistochemistry and electron microscopy 3, 6, 9 and 12 months after surgery.

Results: The nerve endings in the Meissner's corpuscles began to degenerate 3 months after denervation. The elementary structure of Meissner's corpuscles was not significantly altered. Nerve fibers were present around the Meissner's corpuscles, accompanied by growing into its inward. The axons in the denervated nerve disappeared and the Meissner's corpuscles began to atrophy at month 6. More regenerated nerve fibers were observed after nerve implantation, including intensive and thick fibers, accompanied by reinnervation of Meissner's corpuscles. More nerve fibers and a higher proportion of myelinated nerve fibers were noted at month 9 in the implantation group, and the reinnervation was present in the majority of Meissner's corpuscles. Naive myelinated nerve fibers appeared at the caudal end of Meissner's corpuscles. The nerve fibers in the Meissner's corpuscles increased to the normal level at 12 months after nerve implantation.

Conclusions: The implanted nerve regenerated a large amount of free nerve endings, which helped to regenerate simple Meissner's corpuscles via governing previously degenerated corpuscles.

key words: **neurotization • denervated skin • Meissner's corpuscle • nerve fiber • regeneration**

Full-text PDF: http://www.medscimonit.com/fulltxt.php?ICID=882124
Word count: 3369
Tables: –
Figures: 6
References: 36

Author's address: Shi-Rong Li, Department of Plastic Surgery, Southwest Hospital, 3rd Military Medical University, Chongqing 400038, China, e-mail: li1663@yeah.net

Background

Skin flap transplantation is an efficient method to repair wounds and soft tissue defects in clinical practice, whereas the deprived or reduced sensory function is a serious issue after transplantation [1–6]. Whether the sensation is successfully rebuilt or not will directly affect the surgical efficacy and functional recovery in certain sites such as the hand, mouth and penis [7–10].

Sensory nerve implantation has been used to restore the sensory function of denervated flaps [11,12]. Gilbert et al. [13] routinely coapted the pudendal nerve to the major sensory nerves of the donor free flap, and all patients had an encouraging return of tactile and erogenous sensibility. In the study of Fan et al. [14], the regenerated nerves were noted nearby the implanted nerves 2 months after implantation, and at month 4 the flaps were reinnervated by the sensory nerves. Studies also demonstrated flaps can regenerate abundant nerve endings and peripheric receptors in rabbit models [15,16]. However, the mechanisms underlying the reinnervation following implantation are still unknown. For example, how do the nerve endings and tunicate endings regenerate? How is the feeling restored? [17–19].

Generally, there are 4 cutaneous sensations – touch, cold, warm and pain sensations. Nerve endings classified into free nerve endings and tunicate endings (Meissner's corpuscles). Meissner's corpuscle plays an important role in the precise location of sensations. Meissner's corpuscle is a rapidly adaptive mechanical receptor and responsible for sensitivity to light touch with low threshold. It is involved in the 2-point discrimination, which is very important to the normal function of skin. Following peripheral nerve injury, the regeneration of encapsulated nerve endings is critical for the restoration of sensations [20]. Thus, it is imperative to understand the morphological alternations of denervated sensory endings, especially the Meissner's corpuscles, following injury [21].

In the present study, a denervated hand model was established in rhesus monkeys, and the sensory ending degeneration following nerve injury was investigated. In addition, the nerve was implanted into the denervated finger flaps, and immunohistochemistry and electron microscopy were employed to observe the morphological and ultrastructural alternations of the degeneration and regeneration of the sensory endings and Meissner's corpuscles. Electrophysiological testing was performed to determine the type and area of nerve regeneration, aiming to clarify the mechanisms underlying the Meissner's corpuscle regeneration after nerve implantation.

Material and Methods

Animals

Nine rhesus monkeys weighing 4–6 kg, regardless of sex, were purchased from the Experimental Animal Center of the 3rd Military Medical University (Chongqing, China). These monkeys were specific pathogen-free and meet the China National Standard GB14922 (23)-294. This study was carried out in accordance with the guidelines for the care and use of laboratory animals and approved by the ethics committee. Flaps were prepared in a total of 72 2nd-5th fingers. Fingers were randomly divided into 3 groups: normal group (n=5); implantation group (n=5); and non-implantation group (n=5).

Surgical procedures

The monkeys were anesthetized with ketamine (5 mg/kg, IV). A longitudinal incision was made along the midline in each side of the finger, and 2 digital nerves were separated (Figure 1A). In the implantation group, 1 nerve was cut off at the root of the finger, and the proximal end was fixed backward; the other was directly implanted beneath the dermal layer of the flap skin and its end fixed in the sub-derma of the center tip (Figure 1B). In the non-implantation group, both digital nerves were removed at the root of fingers and both ends were also fixed backward (Figure 1C). Finally, the wounds were carefully closed, and the hands were dressed for 1 or 2 days.

Sample collection

The full-thickness skins (1×1 cm) were collected from the finger pulp at the specific time points.

Ultrastructural observation under electron microscope

The samples were fixed in 3% glutaraldehyde and osmic acid for 16 h at 4°C, followed by dehydration in graded ethanol and embedding in epoxy resin. Then, the tissues were consecutively cut into 50 nm-thick sections and double stained by uranyl acetate and sodium citrate. After washing, the sections were examined under a transmission electron microscope.

Immunohistochemistry for neurofilament in the skin tissues

The skin tissues were fixed in 4% paraformaldehyde for 12 h, followed by embedding in paraffin. Then, the 30-μm sections were prepared with a frozen slicer. Streptavidin-peroxidase (SP) method was employed to stain the neurofilament in the skins. Briefly, the sections were deparaffinized, and then washed in distilled water according to the standard protocol. After rinsing in PBST (0.01 M PBS, pH 7.4, KH_2PO_4 0.02%, N_2HPO_4 0.29%, KCl 0.02%, 0.8% NaCl, 0.05% BSA, Tween-20 0.05%, 0.0015% Triton X-100) (3×5 min), sections were treated with 3% peroxide-methanol at room temperature to inactivate endogenous peroxidase. The following steps were carried out in a moist chamber: (1) Incubation with normal goat serum at room temperature for 20 min; (2) Sections were washed with PBST and treated with rabbit anti-human neurofilament antibody (Abcam, USA) (1:200) for 2 h at 37°C; (3) Washing in PBST (3×5 min); (4) Sections were incubated with goat anti-rabbit IgG (Zhongshan Goldenbridge Company, Beijing, China) for 30 min at 37°C; (5) Rinsing with PBST (3×5 min); (6) Sections were incubated with the SA/HRP at 37°C for 30 min; (7) Rinsing in PBST (3×5 min); (8) Visualization by 3, 3-diaminobenzidin (DAB) (Sigma-Aldrich, St. Louis, MO, USA) treatment at room temperature in dark for 10 min; (9) Sections were washed with distilled water and stained with hematoxylin; (10) After dehydration, mounting was performed with neutral gums. The rabbit anti-monkey

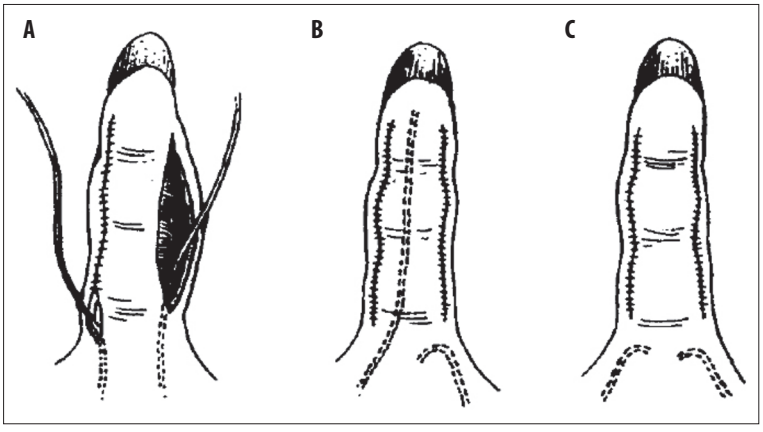

Figure 1. Denervation of the finger skin and nerve implantation. (**A**) The bilateral digital nerves were separated; (**B**) In the implantation group, one digital nerve was cut off at the root of finger and fixed backward, and the other was implanted beneath the dermal layer; (**C**) In the non-implantation group, both digital nerves were cut off at the root of finger and fixed backward.

neurofilament antibody was replaced by PBS in the negative control group. Finally, the sections were imaged using a laser scanning microscope (Olympus Fluoview FV1000, Japan).

The sections were semi-quantitatively scored as previously described. The immunostaining intensity was classified as: no staining (0), mild staining (1), moderate staining (2), and strong staining (3). Grading was performed according to the percentage of positive cells: <5% (0), 6–25% (1), 26–50% (2), 51–75% (3), and >75% (4). The final score of each section was calculated as follows: $score_{intensity} \times score_{grade}$= final score, and the results were expressed as negative (–; 0), weakly positive (+; 1–3), positive (++; 4–7), and strongly positive (+++; 8–12). A minimum of 5 fields were randomly selected from each section for evaluation. The scoring was performed by 2 independent pathologists blind to the study. Any discrepancy was resolved through discussion between the 2 scorers.

Electrophysiological examination

Nerve dissection

Electrophysiological examination was carried out after general anesthesia with ketamine (5 mg/kg, IV) and brachial plexus block at the specific time-points. A 2-3 cm longitudinal incision was made from the root of a finger to the center of the palm, and the proper palmar digital nerve was exposed. The edges of the incision were fixed to form a small bag in which a small quantity of paraffin oil of 37°C was perfused. Then, a single fiber was removed from the nerve trunk with use of a 32X power microscope and a pair of hair-spring tweezers. The proximal end of the single nerve fiber was cut and hung to a platinic electrode connected to the VC-11 electrophysiological system (AZ, USA). The alternations of the waves were recorded using its recorder. The detection was repeated at least 30 times for each digital nerve.

Standards for fiber types

When a responding mechanoreceptor and its afferent single fiber were encountered, the receptive field was located and the absolute response threshold measured with von Frey hair (0.5~100 mN) on its most sensitive point of the receptive field. Then, cold (15°C) and warm (45°C) cotton balls was used as temperature stimuli. The type of this fiber could be identified by the specific adapting behavior. That is to say, the rapidly adapting (RA) fibers respond only to the initiation and discontinuation of 1 or several stimuli, and have no response in continuous skin pressure. However, the slowly adapting (SA) fibers persistently respond to a stimulus for 10 minutes.

Determination of conduction velocity

The conduction velocity of randomly selected fibers was measured in different groups. The electrical stimuli were administered through 2 thin electrodes penetrating into the skin at the most sensitive point of a single fiber's receptive field, and the conduction time between a stimulus and the occurrence of action potential was obtained through the oscilloscope. A stable single-action potential was evoked under a synchronic square-wave stimulus that was 115 times higher than the strength of threshold intensity. The width of the output pulse of electrical stimulator was set at 0.1–0.2 m/s. The distance between the stimulus electrodes to the recording electrode is divided by the conduction time and the results represent the conduction velocity of the fiber.

Statistical analysis

Data are expressed as mean ±standard deviation (SD). Each experiment was repeated at least 3 times. SPSS version 11.0 statistics software was employed to analyze the differences. Analysis of variance (ANOVA) and T test were used to compare the differences among and between groups, respectively. In addition, chi square test and Pearson correlation analysis were also performed. A value of $P<0.05$ was considered statistically significant.

RESULTS

Ultrastructural changes after nerve implantation

Meissner's corpuscles were observed in the dermal papilla layer. The outer membrane was intact and the intermembranous matrix uniform. The diaphragm was arranged spirally, and no non-myelinated nerve fibers were noted. Visible myelinated nerve fibers and Schwann cells were observed at the end of Meissner's corpuscles (Figure 2A, B).

At 3 months after denervation, although the outer membrane of the Meissner's corpuscles was integrated, neural

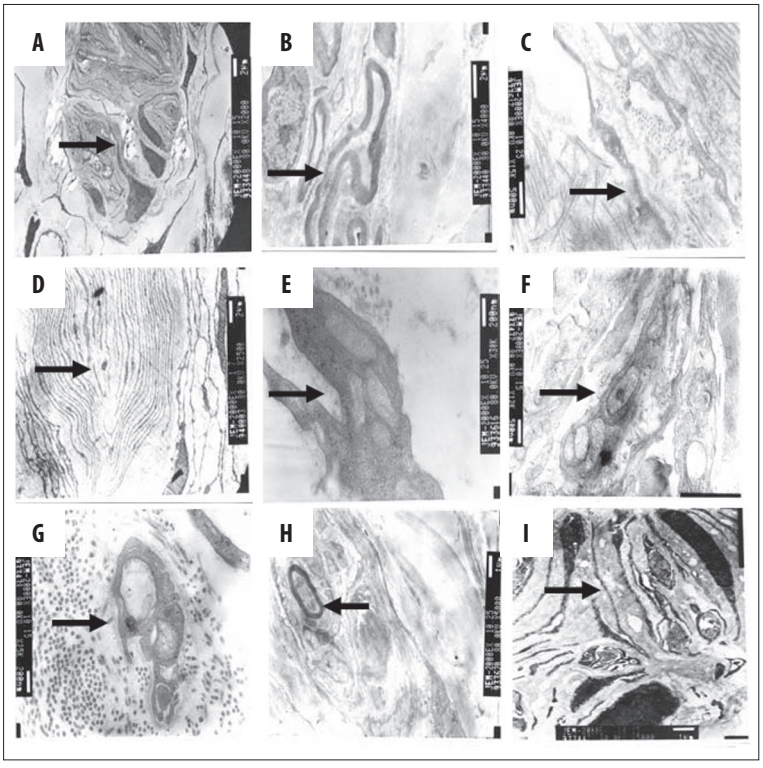

Figure 2. Ultrastructural features after nerve implantation. (**A**) Meissner's corpuscles in the normal group (×2000); (**B**) Nerve fibers in the normal group (×4000); (**C**) Collapsing nerve fibers and ruptured outer membrane with inward collagen growth at month 6 in the non -implantation group (×15000); (**D**) Atrophic Meissner's corpuscles with ruptured outer membrane at month 6 in the non-implantation group (×2500); (**E**) Newly regenerated nerve fibers were present 3 months after nerve implantation (×30000); (**F**) Regenrated nerve fibers began to grow inside the nerve trunk 3 months after nerve implantation (×12000); (**G**) Newly regenerated medullated nerve fibers and nerve trunks occurred 6 months after nerve implantation (×25000); (**H**) Regenrated medullated nerve fibers and nerve trunk occurred 12 months after nerve implantation (×5000); (**I**) Regenerated and integrated Meissner's corpuscles with nearly normal function 12 months after nerve implantation (×5000).

elements began to degenerate, which was mainly characterized by an increased karyoplasmic ratio in Schwann cells at the end of corpuscles, disaggregation or even absence of myelinated fibers, vacuolization of unmyelinated fibers, absence of mitochondria, filaments and microtubules at the axon stump, and formation of cellular tissues.

At 6 months after denervation, the Meissner's corpuscles were degenerated: (1) No further change was present in the corpuscles beside the blood vessels; and (2) Obvious changes occurred in the corpuscles far from the blood vessels. The morphology was disordered, and had a ruptured membrane, increased internal collagen, decreased and dispersed Schwann cells, increased karyoplasmic ratio, integrated cell membrane and nucleus, and completely collapsing endoneurial tubes (Figure 2C, D).

The Meissner's corpuscles began to atrophy at 12 months after denervation, and a large amount of collagen fibers were generated. The contents of corpuscle's Membrane cells and matrix decreased or even disappeared. Schwann cells and their membrane structure disappeared in some Meissner's corpuscles.

Three months after nerve implantation, the outer membrane was integrated and the intermembranous matrix was uniform. Degenerated nerve fibers were seen at the end of corpuscles, whereas the endoneurial tube was integrated and not collapsing. The number of Schwann cells significantly increased in the corpuscles, accompanied by an increase of cytoplasm, decreased ratio of nucleus to cytoplasm, and increase of circular mitochondrial ridge in the cytoplasm. The regenerated non-myelinated nerve fibers appeared around the Meissner's corpuscles near to the blood vessels (Figure 2E, F).

Meissner's corpuscles with simple structure were present at month 6 and were about 1/3~1/2 of normal size. The regenerated corpuscles were located nearby the pre-existing ones. Regenerated axons were found in the center of Meissner's corpuscles. The Meissner's corpuscles had no integrated outer membrane structure, and the content of intermembranous collagen fibers was higher than that normal. Newly regenerated nerve fibers were present, accompanied by a sprouting growth inside the corpuscles (Figure 2G).

Further, the structure of Meissner's corpuscles was improved at 12 months after nerve implantation. One nerve fiber was encapsulated by 2–3 Schwann cells at the end of Meissner's corpuscles, and the regeneration of medullated nerve fibers was also present. The lamellar structure was regularly arranged, and mitochondria, microfilaments and microtubules were seen at the stump of nerve fibers. Two consecutive Meissner's corpuscles were re-innervated by 1 nerve tract. The medullated nerve fibers locating at the end of corpuscles became thicker, and the number of layers increased. The morphology of cells on the membrane was integrated, and the arrangement of membranous lamina regular. The majority of Meissner's corpuscles were mature (Figure 2H, I).

Immunohistochemistry

In the normal group, a small number of uniform dermal nerve fibers were arranged in orderly fashion. Intact Meissner's corpuscles were observed in the dermal papilla. The elliptic or spindle-shaped corpuscles with several layer cells in the center were re-innervated by double or multiple nerve axons. The dermal nerve plexus-derived axons continuously gave out branches after entering into the end of corpuscles, and they spirally traversed among the lamellar cells (Figure 3A, B).

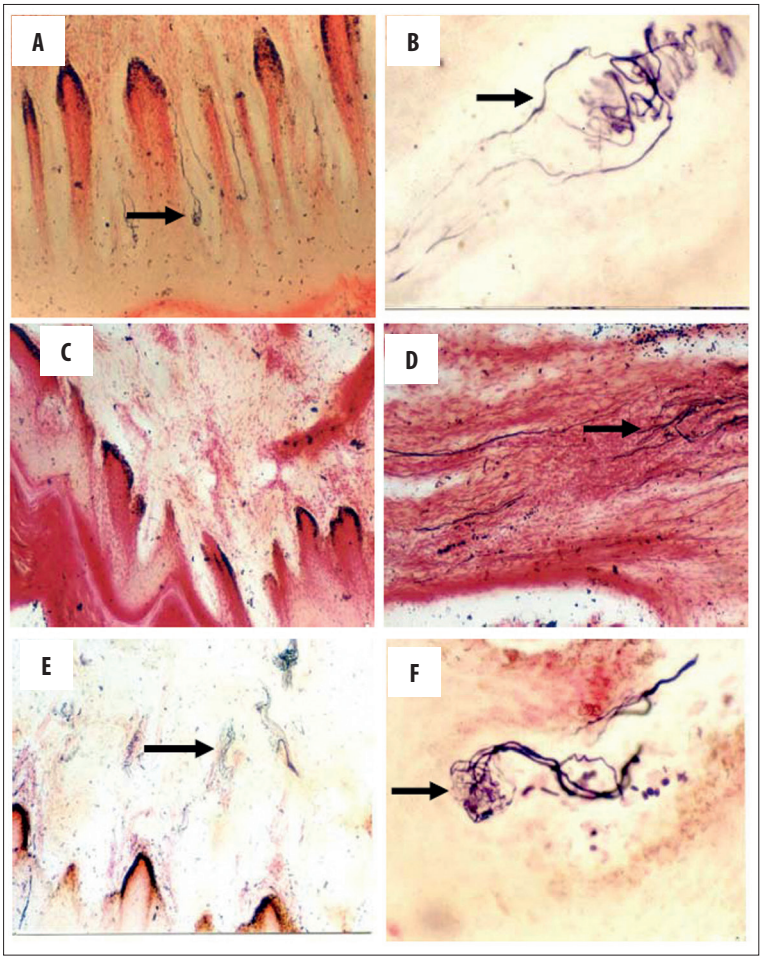

Figure 3. Immunohistochemistry results. (**A**) Distribution of nerve fibers and Meissner's corpuscles in the normal group (SP×100); (**B**) Immunohistochemistry for neurofilament in the Meissner's corpuscles in the normal group (SP×400); (**C**) No regeneration of nerve fibers and Meissner's corpuscles at month 12 in the non-implantation group (SP×100); (**D**) The regenerated nerve fibers in the derma significantly increased 3 months after nerve implantation (SP×100); (**E**) The regenerated nerve fibers significantly increased 6 months after nerve implantation and they grew in a pattern of nerve cluster (SP×100); (**F**) The nearly normal Meissner's corpuscles with increased axon components in the skin regenerated 6 months after nerve implantation (SP×400).

In the non-implantation group, intact skin structure was present, accompanied by small aphthae in some tissues. Germinative positive nerve fibers were occasionally observed in the deep dermis, without obvious regeneration of Meissner's corpuscles (Figure 3C).

The regenerated nerve fibers in the derma significantly increased at 3 months after nerve implantation. The nerve fibers regenerated in a pattern of single fibers and small clusters. Axons were observed in the dermal papilla, accompanied by the regeneration of Meissner's corpuscles. The corpuscles were re-innervated by single axons with less axon component but more collagen fibers (Figure 3D).

The nerve fibers in the derma had regenerated extensively at 6 months after implantation. The number of nerve fibers was higher than that normal and the nerve fibers were distributed intensively. The number of regenerated nerve fiber clusters was increased and the proportion of myelinated fiber was elevated. However, the growth rate of nerve fibers markedly attenuated when compared with that at month 3. The regenerated Meissner's corpuscles significantly increased. These corpuscles had more axon component and fewer collagen fibers re-innervated by multiple axons (Figure 3E, F).

The number of regenerated nerve fibers was maintained at 12 months after nerve implantation (Figure 4A). The regenerated nerve fiber clusters were arranged in order. The proportion of myelinated fibers increased and that of non-myelinated fibers decreased. The number of regenerated Meissner's corpuscles dramatically increased and some were close to the normal corpuscles (Figure 4B). They were mainly re-innervated by multiple axons in a typical helix pattern.

Electrophysiological examination

Nerve trunk implantation increases the number of afferent fibers of mechanoreceptor

In the non-implantation group, the responsive mechanoreceptors appeared only at the region where the proximal end of transected nerve was sutured in the distal palm; very few were found at the proximal palmar nerve of the finger and none were noted beyond the level of the proximal knuckle.

In the normal group and the implantation groups, receptive fields of the re-innervated mechanoreceptors were located regularly from the root to the tip of a finger. To exclude the interference by the growth of regenerated proximal fibers, only a mechanoreceptor whose receptive field was located in the middle and distal phalanx zones was treated as being re-innervated, ensuring that the mechanoreceptor was re-innervated only by the implanted nerve. According to the above criteria, the number of re-innervated mechanoreceptors following nerve implantation was determined

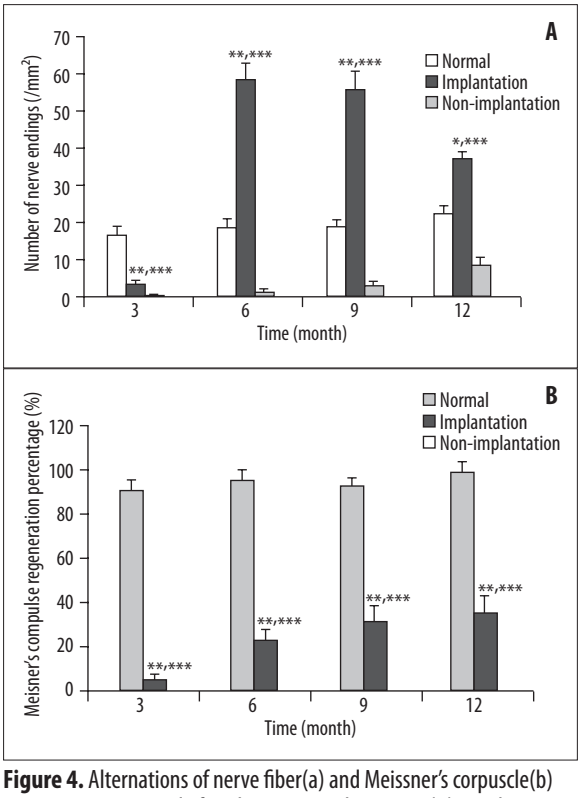

Figure 4. Alternations of nerve fiber(a) and Meissner's corpuscle(b) prior to and after the nerve implantation; (**A**) Number of re-innervated nerve endings in the normal group, implantation group and non-implantation group; (**B**) Percentages of re-innervated Meissner's corpuscles in the normal group, implantation group and non-implantation group. * $P<0.05$, ** $P<0.01$ *vs.* Normal control; *** $P<0.05$ *vs.* Non-implantation.

and expressed as a percentage. The proportion of re-innervated mechanoreceptors rapidly reached up to 47.7% 3 months after nerve implantation. Thereafter, this proportion gradually increased at month 6 and 12. However, the level of re-innervated mechanoreceptors in the implantation group was still lower than that in the normal group 12 months after implantation (Figure 5A).

Proportions of regenerated fast adaptive fiber (RAFs) and slow adaptive fiber (SAFs) mechanoreceptors

The proportion of re-innervated RAFs mechanoreceptors in the implantation group was markedly higher than that in the normal group at months 3 and 6. However, there was no significant difference in the RAFs and SAFs mechanoreceptors 12 months after nerve implantation between the normal group and implantation group (Figure 5B, C).

Alternations of the threshold of re-innervated mechanoreceptors

The mean threshold of RAFs and SAFs were significantly higher in the implantation group than those in the normal group 3 months after nerve implantation. The threshold remained stable 6–12 months after implantation. The mean RAFs threshold reached the near normal level and the SAFs threshold was slightly higher than the normal level at months 6 and 12 (Figure 6).

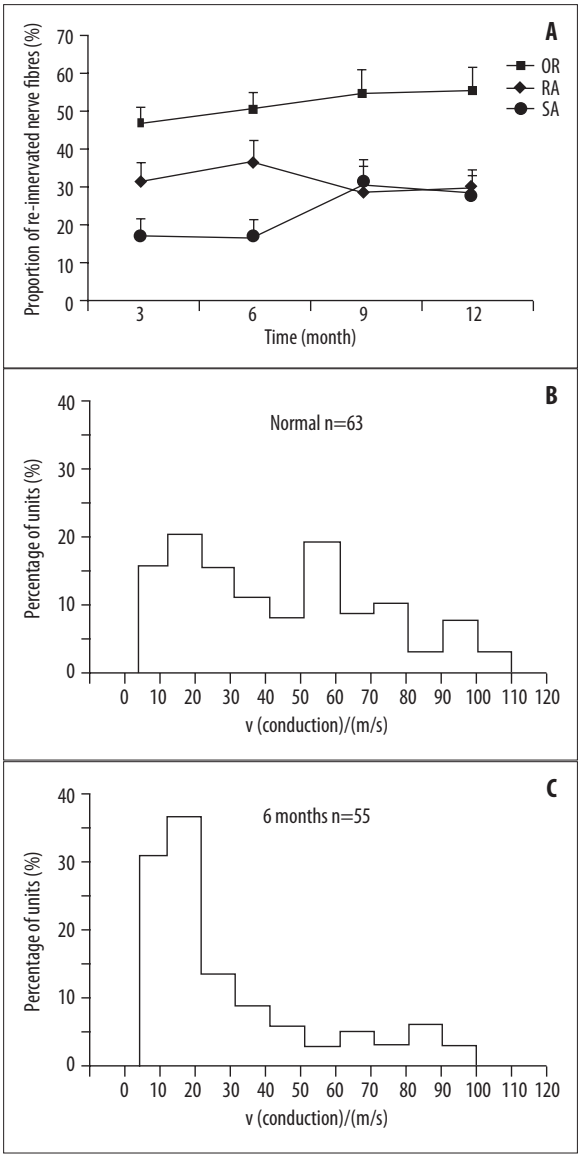

Figure 5. (**A**) the proportion of re-innervated nerve fibers in the afferent nerves of mechanorecepters (%). RA: fast adaptive fiber (RAFs); SA: slow adaptive fiber (SAFs); OR: normal nerve fiber. * $P<0.05$ *vs.* normal nerve fiber; (**B**) Conduction velocity of mechanical fibers in the normal group; (**C**) Conduction velocity for regenerated mechanical fibers at 6 month after the nerve implantation.

Discussion

In the present study we successfully prepared the denervated finger flap in monkeys, and our results revealed that nerve trunk implantation into the denervated flap could promote the nerve regeneration, skin re-innervation and regeneration of Meissner's corpuscles.

Our results showed the Meissner's corpuscles in the denervated hairless skin began to degenerate. The axons ruptured and disappeared, and the endoneurial tubes began to collapse. The theca cells were disrupted and disappeared at month 12, and the Meissner's corpuscles were rich in collagens, but still relatively small [21].

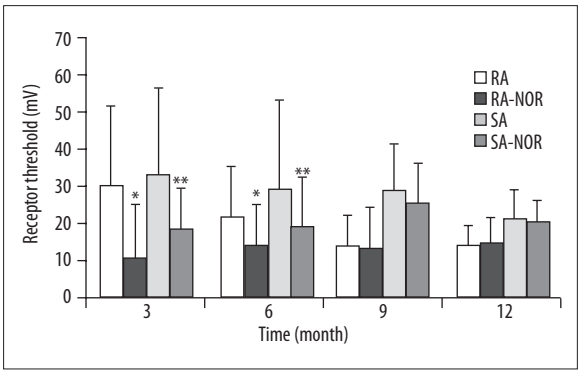

Figure 6. Alternations of thresholds of re-innervated mechanoreceptors * $P<0.05$ *vs.* normal RA, ** $P<0.05$ *vs.* normal SA.

Generally, the degeneration of Meissner's corpuscles is a relatively long process. The nerve degeneration occurred earlier and the development of non-nerve degeneration was prolonged. Interestingly, the nerve implantation group displayed a better nerve restoration when compared with the non-implantation group. Two mechanisms – growth along the endoneurial tube and direct axon growth – might be responsible for the regeneration of Meissner's corpuscles. The process of regenerated Meissner's corpuscle development includes the growth of axons inside the end of corpuscles along the endoneurial tube or repeated sprouting, being packaged by theca cells, and development into the corpuscle body [22,23]. At the early stage, the axons at the terminal part of Meissner's corpuscles were un-myelinated. The myelinated axons were present at month 8, and thickening of medulla sheath and increases of layers were obvious at month 12. The morphology of theca cells was intact and the membranous lamina was arranged regularly, suggesting the Meissner's corpuscles were largely matured. These results strongly suggest that Meissner's corpuscle is a basic structure for sensation. Studies on the degeneration, regeneration, pattern, pathway, and regeneration degree of Meissner's corpuscles will be helpful to further illuminate the mechanism underlying the therapeutic effects of sensory nerve implantation [24,25].

The structure of the implanted skin in the present study was between full-thickness skin graft and transfer of skin flap, which is similar to the structure in the regeneration of skin sensory receptors in clinical practice. Currently, the regeneration of implanted skins with sensation is still controversial [26,27]. The regeneration of implanted nerves is determined by the original skin characteristics, but not the skin receptive field [28]. However, a large number of regenerated Meissner's corpuscles were observed in the implanted palm skin, suggesting that implanted skin can regenerate tunicate receptors [29]. Implanted skin has been found to have both a large number of regenerated nerve endings and considerable regenerated Meissner's corpuscles and epithelium-axon complex. The nerve fibers regenerated and their number finally exceeded that in the normal skin. The process of the development from non-myelinated fibers to myelinated fibers is of great importance to: (1) establish the sensation pathway and provide imprecise sensation as free endings between epidermis and dermis; and (2) provide more opportunities for axons to grow into appropriate terminal organs in a pattern of excessive regeneration. In addition, it interacted with degenerated Meissner's corpuscle and enabled the corpuscle to regenerate, achieving a favorable sensory restoration [30,31].

The results of this study and our previous studies [18,19] show that sensory nerve implantation can achieve good sense reestablishment in the middle- and long-term. Some mechanisms may be responsible for this protective effect: (1) The implanted sensory nerves are mainly thin and have small nerve tracts, and the axonotmesis is far away from the center and near the end. Axonal transection had little effect on the perikaryon, which is beneficial for the nerve regeneration following implantation. (2) The regenerated axons sprouted and inhibition was absent during the process of growth due to anastomosis scar. (3) The regenerated axons may interact with the original degenerated corpuscles or form free endings after growing in or under the derma for a relatively short distance. This shortens the time in degeneration and reduces the degree of degeneration, which are helpful for the reestablishment and restoration of Meissner's corpuscles [32,33].

Conclusions

In conclusion, in the present study we successfully prepared denervated flaps in the fingers of monkeys. Not only a large number of regenerated nerve endings, but also considerable regenerated Meissner's corpuscles were found 12 months after nerve implantation. The number of nerve fibers was higher than in the normal group, and the type of nerve fibers also increased. The gradual regeneration of Meissner's corpuscles suggests a favorable recovery of sensation at the middle- and long-term neurotization [34,35].

Conflict of interest

The authors declare no conflicts of interests.

References:

1. Yu P: Reinnervated anterolateral thigh flap for tongue reconstruction. Head Neck, 2004; 26(12): 1038–44
2. Grasso G, Meli F, Maugeri R et al: Unusual recurrence of trigeminal neuralgia after microvascular decompression by muscle interposal. Med Sci Monit, 2011; 17(4): CS43–46
3. Amr SM, Essam AM, Abdel-Meguid AM et al: Direct cord implantation in brachial plexus avulsions: revised technique using a single stage combined anterior (first) posterior (second) approach and end-to-side side-to-side grafting neurorrhaphy. J Brachial Plex Peripher Nerve Inj, 2009; 19(4): 8
4. Santamaria E, Wei FC, Chen IH et al: Sensation recovery on innervated radial forearm flap for hemiglossectomy reconstruction by using different recipient nerves. Plast Reconstr Surg, 1999; 103: 450–57
5. Vriens JPM, Acosta R, Soutar DS et al: Recovery of sensation in the radial forearm free flap in oral reconstruction. Plast Reconstr Surg, 1996; 98: 649–56
6. Kimata Y, Uchiyarna K, Ebihara S et al: Comparison of innervated and noninnervated free flaps in oral reconstruction. Plast Reconstr Surg, 1999; 104: 1307–13
7. Boyd B, Mulholland S, Gullane P et al: Reinnervated lateral antebrachial cutaneous neurosome flaps in oral reconstruction: Are we making sense? Plast Reconstr Surg, 1994; 93(7): 1350–59
8. Morrison WA, O'Brien BM, MacLeod AM et al: Neurovascular free flaps from the foot for innervation of the hand. J Hand Surg Am, 1978; 3(3): 235–42
9. Mutaf M, Isik D, Bulut O et al: A true one-stage nonmicrosurgical technique for total phallic reconstruction. Ann Plast Surg, 2006; 57(1): 100–6

10. Davis DI, Baratz M: Soft tissue complications of distal radius fractures. Hand Clin, 2010; 26(2): 229–35
11. Narakas AO: Thoughts on neurotization or nerve transfers in irreparable nerve lesions. Clin Plast Surg, 1984; 11(1): 153–59
12. Wu JC, Huang WC, Huang MC et al: A novel strategy for repairing preganglionic cervical root avulsion in brachial plexus injury by sural nerve grafting. J Neurosurg, 2009; 110: 775–85
13. Gilbert DA, Williams MW, Horton CE et al: Phallic reinnervation via the pudendal nerve. J Urol, 1988; 140(2): 295–99
14. Fan QS, Wang CQ, Zhou JG et al: Implantation of sensory nerve into flap: An experimental study and clinical application. Chin J Plast Surg Burns, 1992; 8(3): 193–95
15. Li YJ, Chen SZ, Hu SJ et al: Quantitative study on reestablishment of sensory function after the great auricular nerve being implanted into denervated cervicoshouder flap in rabbits.Chin J Microsurg, 1996; 19(3): 193–96
16. Wang ZX, Chen SZ, Li HY et al: Regeneration of free nerve endings and sensory corpuscles after implantation of nerve into the denervated skin in the monkey. Chin J Plast Surg Burns, 1996; 12(1): 12–14
17. Pearse DD, Pereira FC, Marcillo AE et al: cAMP and Schwann cells promote axonal growth and functional recovery after spinal cord injury. Nat Med, 2004; 10: 610–16
18. Krarup C, Archibald SJ, Madison RD: Factors that influence peripheral nerve regeneration: an electrophysiological study of the monkey median nerve. Ann Neurol, 2002; 51(1): 69–81
19. Walsh SK, Gordon T, Addas BM et al: Skin-derived precursor cells enhance peripheral nerve regeneration following chronic denervation. Exp Neurol, 2010; 223(1): 221–28
20. Vega JA, García-Suárez O, Montaño JA et al: The Meissner and Pacinian sensory corpuscles revisited new data from the last decade. Microsc Res Tech, 2009; 72(4): 299–309
21. Paré M, Albrecht PJ, Noto CJ et al: Differential hypertrophy and atrophy among all types of cutaneous innervation in the glabrous skin of the monkey hand during aging and naturally occurring type 2 diabetes. J Comp Neurol, 2007; 501(4): 543–67
22. Terzis JK, Dykes RW: Reinnervation of glabrous skin baboons: Properties of cutaneous mechanoreceptors subsequent to nerve transection. J Neurophysiol, 1980; 44(6): 1214–25
23. García-Suárez O, Montaño JA, Esteban I et al: Myelin basic protein-positive nerve fibres in human Meissner corpuscles. J Anat, 2009; 214(6): 888–93
24. Paré M, Smith AM, Rice FL: Distribution and terminal arborizations of cutaneous mechanoreceptors in the glabrous finger pads of the monkey. J Comp Neurol, 2002; 445(4): 347–59
25. Calavia MG, Feito J, López-Iglesias L et al: The lamellar cells in human Meissner corpuscles express TrkB. Neurosci Lett, 2010; 468(2): 106–9
26. Alto LT, Havton LA, Conner JM et al: Chemotropic guidance facilitates axonal regeneration and synapse formation after spinal cord injury. Nat Neurosci, 2009; 12(9): 1106–13
27. O'Donnell M, Chance RK, Bashaw GJ: Axon growth and guidance: receptor regulation and signal transduction. Annu Rev Neurosci, 2009; 32: 383–412
28. Michalski B, Bain JR, Fahnestock M: Long-term changes in neurotrophic factor expression in distal nerve stump following denervation and reinnervation with motor or sensory nerve. J Neurochem, 2008; 105(4): 1244–52
29. Dellon AL: Reinnervation of denervated Meissner corpuscles: A sequential histologic study in the monkey following fascicular nerve repair. J Hand Surg, 1976; 1(1): 98–109
30. Kostakoglu N, Manek S, Terenghi G, et al: Free sensate secondary skin flaps: An experimental study on patterns of reinnervation and neovascularisation. Br J Plast Surg, 1994; 47(1): 1–9
31. Mackel R, Brink EE, Wittkowsky G et al: Properties of cutaneous mechanosensitive afferents during the early stages of regeneration in man. Brain Res, 1985; 329(1): 49–69
32. Maria N, Vincenzo P, Claudio C: Quantification of Myelinated Endings and Mechanoreceptors in Human Digital Skin. Ann Neurol, 2003; 54: 197–205
33. Chicarilli ZN, Price GJ: Complete plantar foot coverage with the free neurosensory radial forearm flap. Plast Reconstr Surg, 1986; 78(1): 94–101
34. Shahryar N, Mahmood A, Rasham R et al: Neuronal regeneration in denervated muscle following sensory and muscular neurotization. Acta Orthopaedica, 2008; 79(1): 126–33
35. Stephen WP, Kemp, Jacob A et al: Behavioural and anatomical analysis of selective tibial nerve branch transfer to the deep peroneal nerve in the rat. Eur J Neurosci, 2010; 31: 1074–90